ISSN (Print) 1226-1750
ISSN (Online) 2233-6656
**Journal of Magnetics** 23(3), 370-374 (2018) https://doi.org/10.4283/JMAG.2018.23.3.370

# The Usefulness of Simultaneously Excited Magnetic Resonance Signals from Diffusion Tensor Image

**Kwan-Woo Choi[1], Ho-Beom Lee[1], Soon-Yong Son[2], and Mi-Ae Jeong[3]***

*[1]Asan Medical Center, 88, Olympic-ro 43-gil, Songpa-gu, Seoul 05505, Republic of Korea*
*[2]Wonkwang Health Science University, 514, Iksan-daero, Iksan-si, Jeollabuk-do 54538, Republic of Korea*
*[3]Department of Dental Hygiene, Kangwon National University, Samcheok 25913, Republic of Korea*

(Received 23 May 2018, Received in final form 27 August 2018, Accepted 27 August 2018)

**Clinically acceptable scan time is very important in DTI which is essential for neurologic imaging and there have been ongoing efforts to make the scan time faster. Multi-Band SENSE simultaneous multi slice, also called multiband, is a better solution to reduce scan time. In order to compare the performance of SENSE and MB-SENSE on DTI acquisitions images were acquired using ACR phantom with factor 2 on both groups. The MB-SENSE group showed lower SNR values of center and peripheries than the SENSE in slice 7 (8.78 % and 8.99 % respectively). However, SNR loss is minimal. The SNR values profiles showed a equality from the center to peripheries of the image slice at both MB-SENSE and SENSE. The difference of SNR profiles was approximately 3 % at the center and 9 %-15 % at peripheries at SENSE. This became 3 % at the center and 10 %-15 % at peripheries at MB-SENSE. Therefore, this study has studied and verified the effect of MB-SENSE in temporal resolution over SENSE which are applied on DTI technique using ACR QA program.**

**Keywords :** Parallel imaging, Sensitivity encoding (SENSE), Multi-band SENSE

## 1. Introduction

Typical magnetic resonance image (MRI) acquisition times for whole brain coverage amount to several minutes for a single imaging volume. Within the last few decades, with the implementation of partially parallel imaging (PPI) and techniques such as sum-of-squares reconstruction the noise in MR images does not follow this distribution. PPI involves the use of phased array coils and the acquisition of fewer phase encoding (PE) steps in order to reduce scan time [1, 2]. especially, most common used method in echo planar imaging (EPI). However, As long as MR imaging has existed, there have been ongoing efforts to make it faster. Simultaneous multi slice, also called multiband, is a better solution to reduce scan time a different approach combines slice excitation at different off-resonance frequencies with demultiplexing based on spatial sensitivity differences of RF (Radio Frequency) receiver coils. This method is known as multi-band (MB) SENSE [3-5].


*Corresponding author: Tel: +82-33-540-3391
Fax: +82-33-540-3399, e-mail: teeth2080@kangwon.ac.kr

Using MB-SENSE to excite multiple slices at the same time and then acquire the slices simultaneously can speed up scanning. The MB method allows 2 or more slices to be simultaneously excited, increasing imaging efficiency. The MR signals from MB slices are unfolded by using spatial sensitivity information in each RF channel similar to techniques employed in parallel imaging. Therefore, The SENSE and MB-SENSE methods are not mutually exclusive, and can be combined for improved results.

Therefore, this study has studied the best signal by applying DTI technique, which is the most typical EPI sequence, with SENSE and MB-SENSE.

## 2. Background

Using so-called wide-band or multi-band pulses, it is possible to excite multiple slices simultaneously, as illustrated in the figure. after exciting and acquiring two slices at the same time, the signal measured afterwards is the combination of signals from both slices, so that the resulting image will be the sum of both slices [3]. Applying a SENSE unfolding algorithm allows calculation of the separate images. However, this unfolding can be difficult when coil sensitivity profiles are similar for the


**Fig. 1.** (Color online) Multi-band Sensitivity (MB-SENSE) imaging. A complex RF-pulse simultaneously stimulates two slices, which are phase offset from one another by an amount that depends on the phase-encoding step (here 180°).

two slices, for instance when the distance between slices is small and slices have little difference in geometry factor (g-factor) [6]. To make unfolding the images easier, a phase shift is applied between the slices during the simultaneous excitation 1, 2. This phase shift increases the distance between aliasing voxels, which facilitates unfolding. For FFE type of images, a phase shift between the slices can be obtained by alternating the phase of the excitation pulses for each k-space line 1. For example, by switching the excitation pulse 180° for every second line in k-space, a shift of a half FOV is introduced in one of the images [7]. For single shot EPI acquisitions this approach is not possible, as the entire slice is acquired in a single shot. Therefore, for EPI type of acquisitions gradient blips are played out to achieve a shift. When applying parallel imaging methods such as SENSE, it is important to consider how SNR is affected [8]. As SNR is proportional to the square root of the number of data points, for normal SENSE acquisitions SNR is reduced by a factor equal to the square root of the acceleration factor R. In addition, SNR depends on the g-factor of the coil setup used, as represented in the formula below. With MB- SENSE all data is acquired, so there's no intrinsic penalty on SNR because of the acceleration factor. Only g-factor penalties remain [9]. However, as a result of the slice shifting, the g-factor is more favorable compared to plain SENSE, which implies only a very limited impact on SNR.

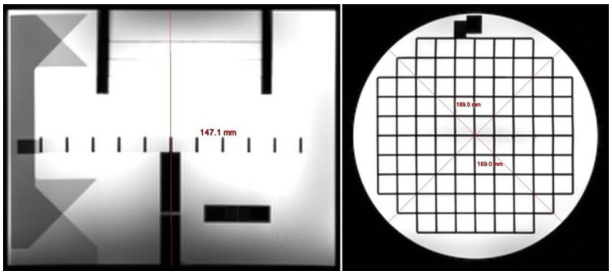


**Fig. 2.** (Color online) A quality assurance method for geometric accuracy measurement.

## 3. Materials and Methods

### 3.1. Image acquisition

For quality assurance of the study method ACR phantom images were evaluated and obtained before and after applying MB-SENSE technique. And then for comparison, Standard axial SE T1 images were obtained using "Phantom Test Guidance for the ACR MRI accreditation program" [10].

The ACR phantom (J10470, J.M specialty, San Diego, Calif.) The ACR MRI phantom was filled with a solution containing 10 mM $NiCl^2$ and 75 mM NaCl. The inner length of the ACR MRI Phantom was 148 mm, and the inner diameter was 190 mm. All experiments were performed using 3.0T scanners (Ingenia CX 3.0T; Philips Medical Systems, Netherlands) equipped with a 32-channel SENSE head coil.

In order to compare the performance of DTI acquisitions with different MB-SENSE factor, DTI was performed using the following protocol: FOV, 250 × 250; matrix size, 128 × 128; slice thickness 5 mm, repetition time (TR) and echo time (TE) shortest, diffusion encoding direction 32 at b = 1000 seconds/$mm^2$, number of excitations, 1; and flip angle, 90 degrees, SENSE factor 2.0 or MB-SENSE factor 2.0.

### 3.2. Image Evaluation

We analyzed the signal to ratio, geometric accuracy, slice-position accuracy, and percent signal-ghosting according to the ACR guidance. For the quantitative analysis of the phantom data, we used the console program of the Philips 3.0T MRI system (software version: Release 5.1.7). The SNR analysis was performed on the registered data at the location of ACR slice 7, where the phantom is uniform. The noise level was measured from the high-b-value images. The SNR of nine circular regions of interest (ROIs), each with a radius of 10 mm, were measured.

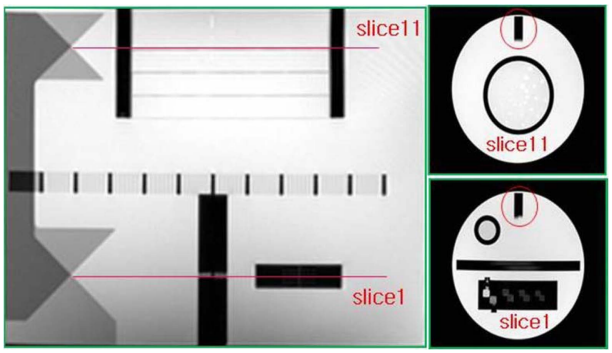


**Fig. 3.** (Color online) A quality assurance method Slice position accuracy measurement.


**Fig. 4.** (Color online) A quality assurance method percent signal ghosting measurement.

This method used a single image to find signal and the non-signal image to find the noise. The average of an ROI encompassing 75 % of the signal producing volume of one of the acquired signal producing images was used as the signal. The noise computation was performed using data from the non-signal-producing image. On the MRI system used in this study, the signal was eliminated by setting the transmit RF coil voltage to 0 V. The standard deviation of the ROI with the same geometry used to compute the signal was then measured on the non-signal image and divided by 0.66 [11]. The SNR is determined by:

$$\text{SNR} = \frac{S}{\textit{image noise}}$$

The geometric accuracy and the slice-position accuracy were measured at b = 0 images of 32 directions. The diameter of the phantom was measured in four directions: top-to-bottom, left-to-right, and both diagonals. The slice-position accuracy was measured at slices 1 and 11 of the b = 0 images of DTI. The scans were performed such that slices 1 and 11 passed the crossing point in the middle of 45° wedges, and the slice-position accuracy was measured by using the difference in lengths between a pair of black vertical rods. When the scan was taken above the crossing of wedges, the rod on the right side appeared longer in the image. Conversely, when it was taken below the crossing point of wedges, the rod on the left appeared longer in the image.

To evaluate percent signal-ghosting, we placed a large round ROI between with an area 195 $cm^2$ and 205 $cm^2$ in the middle of the phantom. Also, there are four ROIs in the four edges of the field of view (FOV). Each ROI has an area of about 10 $cm^2$ and a length-to-width ratio of about 4 : 1. The ROIs were labeled top, bottom, left, and right. The percent signal-ghosting ratio was calculated using the following formula:

$$\text{Ghosting ratio} = \frac{(\text{top} + \text{bottom}) - (\text{left} + \text{right})}{2x(\text{large ROI})}$$

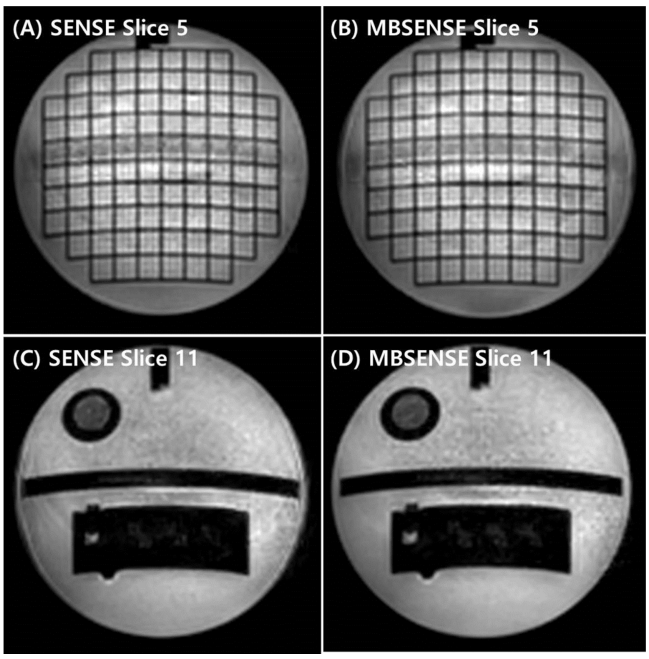


**Fig. 5.** Sensitivity (SENSE) and Multi-band Sensitivity (MB-SENSE) imaging.

### 3.3. Statistical Analysis

The statistical significance of the parametric data was determined using a paired sample t test. A two-sided P value less than 0.05 was considered to indicate statistical significance. All statistical analysis was performed using the SPSS software package (version 18; SPSS, Chicago, IL, USA).

## 4. Results

The image obtained from MB-SENSE showed lower SNR values of center and peripheries than the SENSE in slice 7 (8.78 % and 8.99 % respectively). However, SNR loss is minimal. The SNR values profiles showed an equality from the center to peripheries of the image slice at both MB-SENSE and SENSE. The difference of SNR profiles was approximately 3 % at the center and 9 %-15 % at peripheries at SENSE. This became 3 % at the center and 10 %-15 % at peripheries at MB-SENSE. The

**Table 1.** Quantitative results of SNR in two groups.

| Category | | SENSE | MB SENSE | P value |
|---|---|---|---|---|
| SNR | Circle-center | 312.75 ± 9.37 | 297.56 ±8.65 | .248 |
| | Left side | 256.60 ± 8.48 | 230.87 ± 9.14 | .562 |
| | Right side | 263.45 ± 10.23 | 239.53 ± 9.88 | .478 |
| | Upper side | 289.82 ± 12.86 | 265.46 ± 9.32 | .425 |
| | Lower side | 241.65 ± 9.28 | 228.79 ± 8.72 | .378 |

results of the qualitative analysis are summarized in Table 1.

ACR phantom test measurements in this study did not meet this passing standard. There were statistically no significant differences in the geometric accuracy, slice-position accuracy, and percent signal-ghosting between the MB-SENSE and SENSE applying DTI technique all scan directions. The results of testing on the two technique are summarized in Table 2-4.

In the geometry accuracy analysis, the top-to-bottom diameters had a 178.91 mm error in SENSE and a 179.72 mm error in MB-SENSE while Rt-diagonal diameters had 186.85 mm and 186.47 mm errors, and the Lt-diagonal diameters had 186.54 mm and 186.63 mm errors at SENSE and MB-SENSE, respectively. and in the slice position accuracy analysis, above slice 1 the crossing of wedges diameter difference had a 5.42 mm and 5.48, below slice 11 the crossing of wedge diameter difference had a 5.09 mm and 5.20 mm. Additionally, percent signal-ghosting tests were significant in all directions, With

**Table 2.** Quantitative results of geometric accuracy in two groups.

| Category | | SENSE | MB SENSE | P value |
|---|---|---|---|---|
| Geometric accuracy (mm) | Top-to-bottom | 178.91 ± 0.93 | 179.72 ± 0.95 | < 0.001 |
| | Left-to-Right | 184.37 ± 0.88 | 185.19 ± 0.96 | < 0.001 |
| | Rt-diagonal | 186.85 ± 0.91 | 186.47 ± 0.76 | < 0.001 |
| | Lt-diagonal | 186.54 ± 0.79 | 186.63 ± 0.79 | < 0.001 |

**Table 3.** Quantitative results of slice position accuracy in two groups.

| Category | | SENSE | MB SENSE | P value |
|---|---|---|---|---|
| Slice-position accuracy (mm) | Slice 1 | 5.42 ± 0.26 | 5.48 ± 0.21 | < 0.001 |
| | Slice 11 | 5.09 ± 0.33 | 5.20 ± 0.35 | < 0.001 |

**Table 4.** Quantitative results of percent signal-ghosting in two groups.

| Category | SENSE | MB SENSE | P value |
|---|---|---|---|
| Percent signal-ghosting (%) | 4.39 ± 0.75 | 4.77 ± 0.69 | < 0.001 |

**Table 5.** Scan time results of DTI image in two methods.

| Category | scan time |
|---|---|
| SENSE DTI | 2 min 13 sec |
| MBSENSE DTI | 1 min 09 sec |

regard to percent signal ghosting, the ACR passing standard was ghosting ratio less than 0.025 (2.5 %). The DTI images from standard T1 had a ghosting ratio less than 0.025 (2.5 %) while SENSE and MB-SENSE had a ghosting ratio greater than 0.045 (4.5 %).

## 5. Discussion

DTI is a well-established method for neurologic application [12-15]. Clinically acceptable time is very important as its sound pressure level is significantly higher than other sequences. Also quality assurance is essential as DTI is affected by numerous technical factors and it is not yet standardized among vendors. In previous study, Wang *et al.*, noted SNR, distortion and deviation of images are key components of DTI QA program. As adequate SNRs and reliable diffusion tensor quantification and minimum distortion are required, we verified the image quality by following NEMA guidance calculating SNR and ACR guidance measuring distortions and deviations.

Setsompop *et al.*, verified simultaneous multi-slice echo planar imaging imposes penalty on g-factor penalty sacrifices on SNR (10). Todd *et al*., noted false signal on higher MB factors using 2D multiband EPI imaging for high-resolution, whole-brain, task-based fMRI studies at 3T. In our study to minimize those penalties on g factor, SNR and reduce false positive signals, MB factor and SENSE factors were set to minimum 2.

MBSENSE technique has an advantage over SENSE as the scan time significantly reduces from to more significantly than has been previously shown, while not significantly sacrificing spatial resolution or SNR as the multiband (MB) radiofrequency (RF) simultaneously excite and acquire multiple slices.

Another advantage of MBSENSE is that The SNR values profiles showed a equality from the center to peripheries of the image slice at both MB-SENSE and SENSE.

In our study, this study measured MB-SENSE compared to SENSE technique compared to partial SENSE parallel technique to reduce scan time while maintaining SNR on depicting DTI sequence.

The minimum MB factor 2 appeared reasonable and clinically applicable as there are statistically no significant

differences in the geometric accuracy, slice-position accuracy, and percent signal-ghosting between the MB-SENSE and SENSE applying DTI technique all scan directions.

However, commercial DTI uses SENSE reconstruction with Cartesian sampling of k-space which could be challenging for time reduction due to its high computation complexity [16].

Our study result suggests that in combination with MB factor 2, a directly proportional improvement in temporal resolution is offered while SNR loss is not significant.

As a result of research, we found that a ACR measurement method using a multi-channel coil and a parallel imaging technique shows the lowest relative standard deviation both in SENSE and MB-SENSE DTI images, and thus shows a high degree of precision.

Our study has some limitations. Firstly, previous several researches [4, 13, 16-18] have already presented replaceable multiband methods for supplementing limits of the SENSE method and for measuring more accurate MR data. However, multiband methods have not yet optimized and this study tested a new combination of MB-SENSE factor 2 and SENSE factor 2. Also, each of previously proposed methods also had limits and requirements on reconstitution methods. Secondly, imaging at high MB factors can lead to false-positive activation arising from signal leaking between simultaneously excited slices when the data is reconstructed with the Slice-algorithm. To prevent or minimize this false positive activation we used the minimal MB-SENSE factor 2.

Thirdly, the phantom used for DTI QA ideally should have built-in anisotropy. Much work has been devoted to design and construct such phantoms. However, such phantom was not available for routine use.

As with all data acquisition acceleration schemes, there is a limit to the amount of under sampling that can be done before significant image artifacts appear. Also, there was a limit to the progress of the present study [4].

In spite of these limitations, the MB-SENSE is advantageous for fast imaging compared to SENSE parallel technique. Thu it is useful for providing fast DTI imaging and it allowed maintaining high-quality image.

## 6. Conclusion

In conclusion, the modified MB-SENSE technique using the parallel method shortens the scanning time and minimizes the image quality in acquisition of the DTI images while it keeps the diagnostic value of the ACR MRI accreditation program.

## References

[1] P. J. Basser, J. Mattiello, and D. Lebihan, Biophys. J. **66**, 1 (1994).
[2] L. Bihan, J. F. Mangin, C. Poupon, C. A. Clark, S. Pappata, N. Molko, and H. Chabriat, J. Magn. Reson. Imaging **13**, 4 (2001).
[3] D. K. Sodickson, U.S. Patent No **5**, 910,728 (1997).
[4] F. A. Breuer, M. Blaimer, R. M. Heidemann, M. F. Mueller, M. A. Griswold, and P. M. Jakob, Magn. Reson. Med. **53**, 3 (2005).
[5] K. Setsompop, B. A. Gagoski, J. R. Polimeni, T. Witzel, V. J. Wedeen, and L. L. Wald, Magn. Reson. Med. **67**, 5 (2012).
[6] M. Blaimer, F. Breuer, M. Mueller, R. M. Heidemann, M. A. Griswold, and P. M. Jakob, Top Magn. Reson. Imaging **15**, 4 (2004).
[7] K. P. Pruessmann, M. Weiger, M. B. Scheidegger, and P. Boesiger, Magn. Reson. Med. **42**, 5 (1999).
[8] J. Haselgrove and M. Prammer, Magn. Reson. Imaging **4**, 6 (1986).
[9] S. Bollmann, A. M. Puckett, R. Cunnington, and M. Barth, NeuroImage, **166**, 155 (2018).
[10] Z. J. Wang, Y. Seo, J. M. Chia, and N. K. Rollins, Medical Physics **38**, 7 (2011).
[11] Association NEM. Determination of signal-to-noise ratio (SNR) in diagnostic magnetic resonance imaging, NEMA standard publication MS (2008).
[12] D. K. Jones, M. A. Horsfield, and A. Simmons, Magn. Reson. Med. **42**, 3 (1999).
[13] S. Skare, M. Hedehus, M. E. Moseley, and T. Q. Li, J. Magn. Reson. **147**, 2 (2000).
[14] S. M. Smith, M. Jenkinson, H. Johansen-Berg, D. Rueckert, T. E. Nichols, C. E. Mackay, K. E. Watkins, O. Ciccarelli, M. Z. Cader, P. M. Matthews, and T. E. J. Behrens, NeuroImage **31**, 4 (2006).
[15] P. C. Sundgren, Q. Dong, D. Gomez-Hassan, S. K. Mukherji, P. Maly, and K. Welsh, Neuroradiology **46**, 5 (2004).
[16] E. Dai, X. Ma, Z. Zhang, C. Yuan, and H. Guo, Magn. Reson. Med. **77**, 4 (2017).
[17] N. Todd, S. Moeller, E. J. Auerbach, E. Yacoub, G. Flandin, and N. Weiskopf, Neuroimage **124**, 32 (2012).
[18] D. A. Feinberg, T. G. Reese, and V. J. Wedeen, Magn. Reson. Med. **48**, 1 (2002).
[19] D. A. Feinberg, S. Moeller, S. M. Smith, E. Auerbach, S. Ramanna, M. Gunther, M. F. Glasser, K. L. Miller, K. Ugurbil, and E. Yacoub, PLoS One **5**, 12 (2010).